Available online at www.sciencedirect.com
ScienceDirect
ELSEVIER
International Journal of Rock Mechanics & Mining Sciences 44 (2007) 787–801
International Journal of Rock Mechanics and Mining Sciences
www.elsevier.com/locate/ijrmms

The relationship between closure pressures from fluid injection tests and the minimum principal stress in strong rocks

Emma J. Nelson[a,*], Simon T. Chipperfield[b], Richard R. Hillis[a], John Gilbert[b], Jim McGowen[c], Scott D. Mildren[d]

[a]*Australian School of Petroleum, The University of Adelaide, Australia*
[b]*Santos Ltd, Adelaide, Australia*
[c]*Halliburton Australia, Australia*
[d]*JRS Petroleum Research, Adelaide, Australia*

Accepted 17 October 2006
Available online 7 February 2007

Abstract

Closure pressures measured during injection tests such as mini-fracs are normally considered an accurate measure of the minimum in situ principal stress magnitude. This paper presents stress, strength and image log data from the Australian Cooper Basin, which suggests that in reservoirs with high in situ stress, high tensile strength and weak geological fabrics, interpreted closure pressures may be significantly greater than the minimum principal stress.

Closure pressures interpreted from mini-frac injection tests in the Cooper Basin, suggest the minimum principal stress varies from 12.4–27.2 MPa/km (0.55–1.2 psi/ft). To better understand the reasons for this variation in closure pressure, image logs and mini-frac data from 13 treatment zones, and core from seven of these treatment zones, were analysed. The analysis revealed that treatment zones with high measured closure pressures ($\geqslant$18.1 MPa/km; 0.8 psi/ft), high treating pressures ($>$31.6 MPa/km; 1.4 psi/ft) and high measured hydraulic fracture complexity existed in reservoirs with high tensile rock strength ($>$7 MPa; 1015 psi) and geological fabrics (planes of weakness) including natural fractures. Conversely, treatment zones with lower measured closure stress ($\leqslant$19 MPa/km; 0.84 psi/ft) and low hydraulic fracture complexity occurred in reservoirs with lower tensile strength and/or no geological fabrics.

We suggest that closure pressures in rocks with high tensile strength and weak geological fabrics may not be representative of the minimum principal stress magnitude in the Cooper Basin where they are associated with hydraulic fracture complexity. Rather, they reflect the normal stress incident on pre-existing weaknesses that are exploited by hydraulic fluid during the mini-frac injection.

Keywords: In situ stress; Mini-frac injection test; Closure pressure

1. Introduction

Accurate knowledge of the in situ stress tensor is required in the analysis, planning and/or development of stable petroleum well trajectories, secondary oil and gas recovery, sand control, pre-conditioning of ore in mining, coal seam methane, gas storage, waste disposal and civil development projects [1,2]. Consequently, much work has gone into developing methods for accurately measuring in situ stress during drilling (e.g., leak-off and extended leak-off tests) and hydraulic fracturing operations (e.g., mini-frac, micro-frac and step-rate injection tests) [3,4]. Most of these methods assume the creation of a simple bi-modal fracture in an isotropic homogeneous rock mass that propagates in the maximum principal stress direction and opens against the minimum principal stress [5].

Stress magnitudes and orientations have been shown to vary between lithologies in petroleum fields [6–8]. It has been proposed that the variation in stress distribution through different lithological units in a sedimentary basin depends on relative rock strength and the present-day

*Corresponding author. Present address: BP Exploration, Chertsey Road, Sunbury-on-Thames, Middlesex TW16 17LN, UK.
Tel.: +44 1932 739521; fax: +44 1932 738411.
E-mail address: Emma.Nelson@bp.com (E.J. Nelson).

1365-1609/$ - see front matter © 2007 Elsevier Ltd. All rights reserved.
doi:10.1016/j.ijrmms.2006.10.004

state-of-stress [9,10]. This concept of 'stress partitioning' can account for some variation in minimum horizontal stress as measured by leak-off tests and mini-frac injections.

Cornet and Valette [11] observed that hydraulic fractures often propagate along pre-existing planes of weakness in crystalline rocks and showed that when pre-existing planes of weakness are not normal to S_{hmin}, hydraulic fracturing can be dominated by these planes and closure pressures can reflect the magnitude of the normal stress supported by the plane [11]. Similarly, Iverson [12] showed that hydraulic fracture closure pressures are dependent on tensile strength and do not necessarily measure the minimum horizontal stress. Iverson [12] demonstrated that when tensile strength anisotropy is greater than the difference between the intermediate and minimum principal stress magnitudes, the induced hydraulic fracture can open perpendicular to the intermediate stress direction [12].

Following on from these previous studies, this paper reviews the stress tensor, mini-frac pressure records, prevailing rock fabrics and the tensile strength of the reservoir rock to assess the accuracy of pump-in tests to determine S_{hmin} in the Cooper Basin. Thirteen treatment zones were analysed in which image logs and hydraulic fracture pressure-records were available. Tensile rock strength testing was undertaken on core from seven of the treatment zones.

2. The in situ stress tensor in the Cooper Basin

Several studies have been undertaken to determine the in situ stress tensor in the Cooper Basin [13–15]. Here we summarise previous relevant studies to constrain the magnitudes of the minimum horizontal stress, vertical stress and the orientation and magnitude of the maximum horizontal stress in the Cooper Basin. In the following section, we discuss the methodology used herein to estimate S_{hmin} from injection tests with specific reference to the Cooper Basin.

2.1. Vertical stress magnitude

The vertical stress has been shown to vary considerably across the Cooper Basin [14]. Vertical stress profiles determined by Reynolds et al. [14] indicate that vertical stress ranges from 16.8 MPa/km (0.75 psi/ft) to 19.8 MPa/km (0.87 psi/ft) at 1 km depth and from 59.7 MPa/km (0.88 psi/ft) to 67.8 MPa/km (1 psi/ft) at 3 km depth (Fig. 1). These vertical stress gradients were determined by integrating density logs from 24 wells. Vertical stress calculations require density data from sea-level. The average density from sea-level to the top of the density log can be estimated by converting check shot velocity survey data to average density using the Nafe–Drake velocity/density transform [16]. The variability in vertical stress may be due to variable uplift and exhumation across the Cooper Basin [17] and/or may be due to the variation in the thickness of low-density coals in the Cooper Basin.

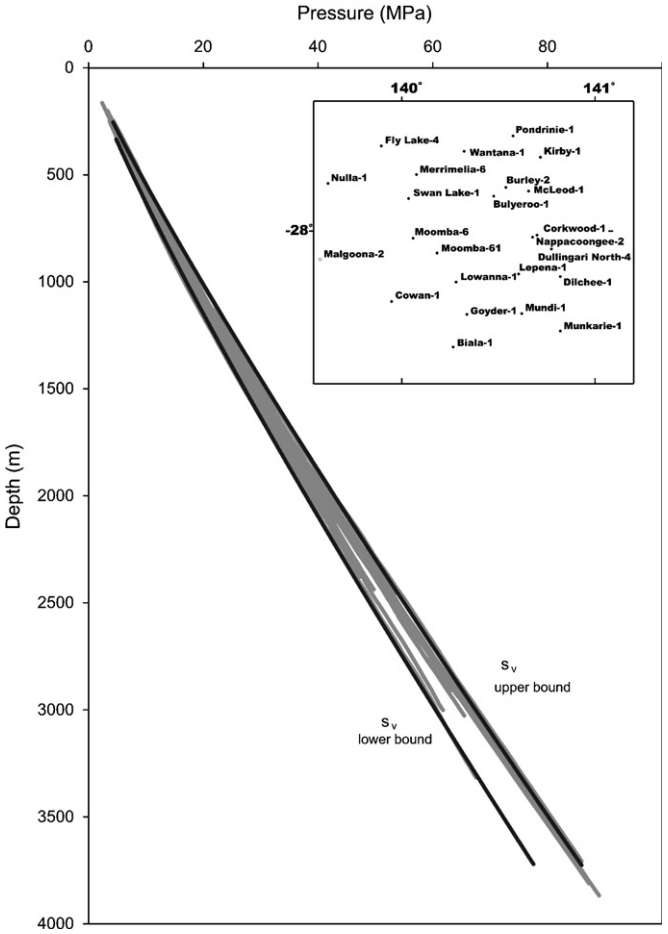

Fig. 1. Vertical stress profiles in the Cooper Basin (from [14]).

2.2. Orientation of the maximum horizontal stress

The orientation of the maximum horizontal stress in the Cooper Basin can be determined using breakouts and drilling-induced tensile fractures (DITFs) observed on image logs and/or caliper logs [15]. The orientation of S_{Hmax} is predominantly east–west (090°N) throughout the Cooper Basin although there appears to be some local stress rotation adjacent to faults (Fig. 2).

2.3. Minimum horizontal stress magnitude

The minimum horizontal stress magnitude can be determined from the lower-bound to leak-off tests [5] or from the closure pressure (P_c) measured during a mini-frac injection test where the fracture formed is vertical and oriented perpendicular to S_{hmin} [5]. Hillis et al. [18] and Reynolds et al. [14] used lower bound to leak-off pressures to constrain the minimum horizontal stress to ~15.5 MPa/km (0.68 psi/ft) in the Cooper Basin [14,18]. Mini-frac injection tests are generally considered a more reliable

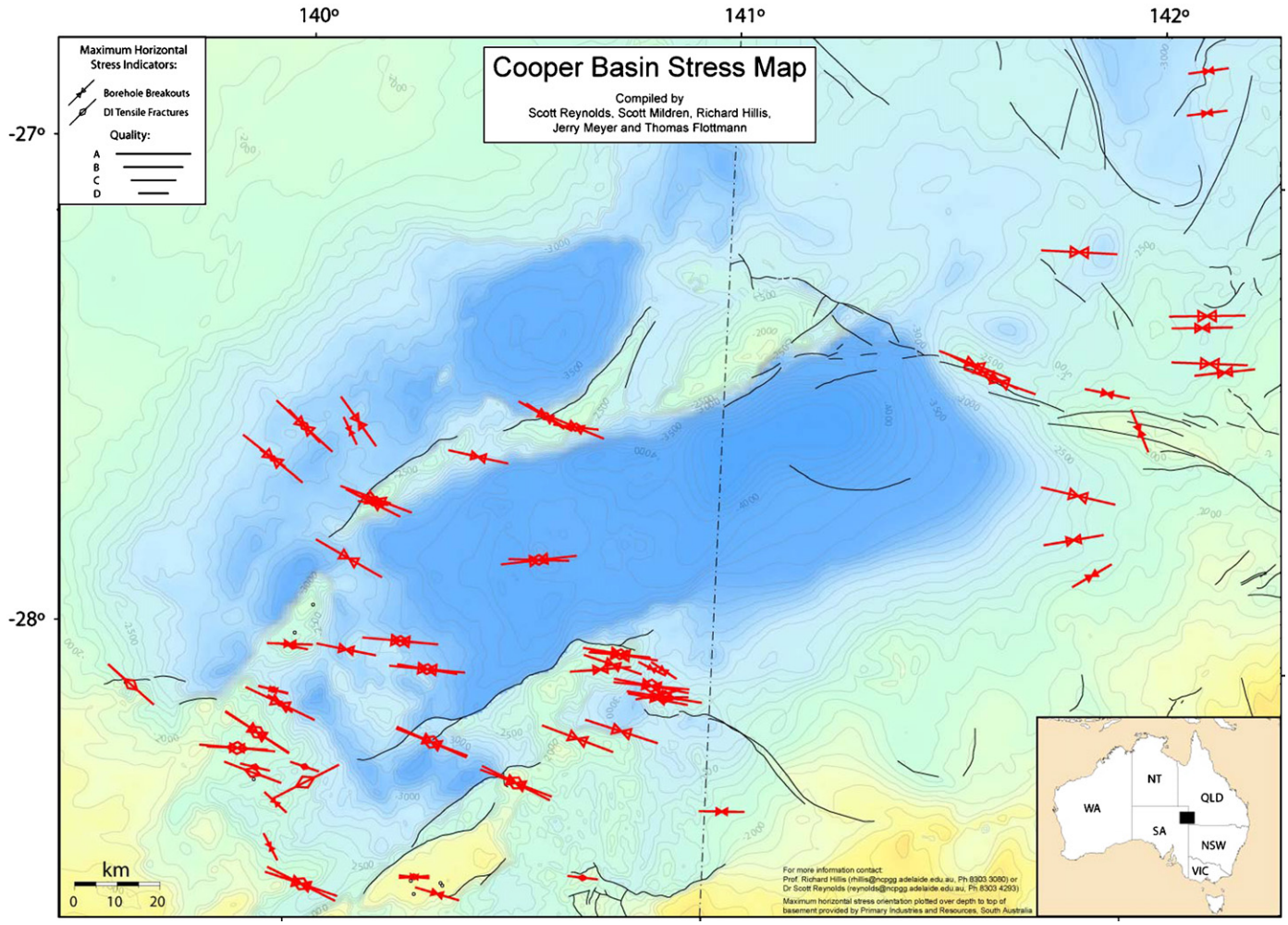

Fig. 2. Orientation of the maximum horizontal stress in the Cooper Basin (from [15]).

means of estimating S_{hmin} than leak-off tests [5,19]. Over 600 mini-frac-type injections have been conducted in the Cooper Basin and analysis of their closure pressures have been shown to range from 13.6 to 24.9 MPa/km (0.6–1.1 psi/ft) [14,20]. Although most authors agree that closure pressures derived from mini-frac injection tests are representative of S_{hmin}, there is some uncertainty regarding how to resolve the P_c from the pressure decline following shut-in [21]. Here we argue that a conventional interpretation of closure pressure often provides an unreliable estimate of minimum horizontal stress in the Cooper Basin, and methodologies used to interpret mini-frac injection tests and their limitations are discussed in the next section of this paper.

2.4. Maximum horizontal stress magnitude

The S_{Hmax} magnitude can be determined using frictional limit theory [14,22] or where breakouts or DITFs are observed on image logs and where the compressive rock strength or tensile rock strength is known [14,23,24]. Reynolds et al. [14] used frictional limit theory and the observation of DITFs to constrain the S_{Hmax} magnitude to 38.8–40.8 MPa/km (1.71 psi/ft–1.80 psi/ft) in Dullingari North 8, and 37.9–38.6 MPa/km (1.67–1.71 psi/ft) at Bulyeroo 1 in the Cooper Basin. However, these approaches require the magnitude of S_{hmin} to be well constrained, and the rock strength to be known. We suggest that closure pressures measured from mini-frac injections in the Cooper Basin are not a true reflection of the S_{hmin}. We use rock strength data that was not available to Reynolds et al. [14], and an alternative method of Nelson et al. [25], to constrain S_{Hmax} in the Cooper Basin without the use of mini-frac closure pressures (Appendix). We determine a lower bound to S_{Hmax} of 41.9 MPa/km (1.85 psi/ft) in the Cooper Basin.

3. Estimating the closure pressure from injection tests in the Cooper Basin

The most reliable estimate of S_{hmin} is yielded by injection tests including mini-frac (pump-in/flow-back, pump-in/shut-in) tests and micro-frac tests [5,19]. These tests involve injecting fluid at high rate (typically in excess of 10 bpm)

so that it creates a hydraulic fracture that propagates a considerable distance from the well bore wall into the formation rock. After the hydraulic fracture is created, and pumping has continued at a constant rate to allow the fracture to propagate, the well is shut-in and the subsequent pressure decline is analysed. All mini-fracs considered herein were undertaken in cased and cemented well bores through perforations.

The pressure decline following a mini-frac injection provides a continuum of information about the near-well bore and far-field behaviour of the hydraulic fracture (simple versus complex propagation) and of the far-field reservoir itself (Fig. 3; [26–28]). An initial, sudden pressure drop after shut-in identifies near well bore restrictions (complexity) often called near well bore pressure loss (NWBPL; [26,29]). The pressure at the end of the early-time (rapid) pressure decline period is defined as the 'instantaneous shut-in pressure' (ISIP) or colloquially the 'frac gradient' when normalised for reservoir depth. A high ISIP may indicate complex hydraulic fracture growth close to the well bore. After the early-time pressure drop following shut-in the pressure declines more slowly and the created hydraulic fracture continues to close (the pre-closure period) until finally mechanical closure is reached (P_c, Fig. 3). The value, P_c, is generally considered equivalent to the minimum horizontal stress, S_{hmin}. The difference in pressure between the ISIP and P_c is defined as the net pressure (P_{net}) at shut-in or the pressure drop along the length of the created fracture at shut-in [27]. A large difference between the ISIP and P_c (i.e., a high P_{net}) is believed to represent complex hydraulic fracture propagation in the far field (distances greater than three well bore diameters from the well bore wall [30]). Fig. 4 shows pressure and flow rate time series which illustrate the difference between a simple fracture stimulation with low treating pressure (A; B6 well) and a complex treatment with a high treating pressure (B; B54 well). After the fracture closes, the pressure continues to decline at a rate which is dictated by the reservoir properties only and transitions through pseudo-linear and pseudo-radial flow regimes before stabilising at reservoir pressure [31].

Although most authors agree that closure pressures derived from mini-frac injection tests are representative of S_{hmin}, there are many methodologies used to determine P_c from the pressure decline following shut-in [21]. Early methods of identifying P_c from mini-frac injections utilised the square root of shut-in time or the square root of the sum of shut-in time and injection time to identify significant flow regime changes during the pressure decline [28,32]. However, the technique used herein uses a plot of pressure as a function of pressure versus G-time [33,34]. The G-time function was constructed to account for the temporal and spatial variation of leak-off observed in the reservoir as the created hydraulic fracture propagates and recedes [35,36]. On a plot of pressure versus G-time the pre-closure time period is linear for ideal, simple (constant compliance) fracturing cases (Fig. 5; [28,32]). While the G-Function was originally derived for this limiting case, Nolte [37] later discussed the impact of non-ideal (complex) fracture propagation behaviour such as fracture extension during closure, height recession and pressure-dependent fluid loss (fluid loss controlled by natural fractures or fissures that dilate during injection) on the G-function plot [37]. We use the approach of Barree and Mukherjee [36], which follows Nolte [37] to interpret hydraulic fracture complexity (non-ideal behaviour) on G-function (derivative and superposition derivative) plots. Some examples of the methodology used to identify hydraulic fracture complexity are depicted in Fig. 5 [38]. It should be noted that mini-frac pressures were recorded by down-hole pressure gauges in all tests considered herein.

Despite careful assessment of mini-frac pressure declines using the above-mentioned method, fracture closure was still difficult to define in some instances in the Cooper Basin. G-function plots for mini-frac injections in two Cooper Basin wells are displayed in Fig. 6. Fig. 6A is an example of fracture closure that is easy to pick from the G-function derivatives and Fig. 6B is an example of where fracture closure was more difficult to determine. Analysis of closure pressures from mini-fracs in reservoirs of hydrostatic pressure in this study revealed that they ranged from 12.4 to 27.2 MPa/km (0.55–1.2 psi/ft) (Fig. 7). This interpretation is consistent with previous studies undertaken in the Cooper Basin [14,20]. As is discussed subsequently in this paper, we do not believe this range in P_c really reflects S_{hmin} in the Cooper Basin.

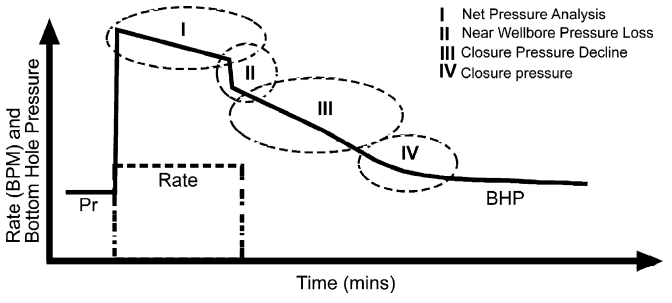

Fig. 3. Information obtained from a typical mini-frac injection in tight rocks. P_r refers to reservoir pressure and BHP to bottom hole pressure.

4. Rock fabrics in the Cooper Basin

Image logs covering the 13 treatment zones studied herein were interpreted to determine if there is a relationship between hydraulic fracture complexity observed during the pumping of mini-fracs and geological weaknesses (complexity) inherent in the reservoir. Image logs produce a 3D resistivity 'image' of the well bore wall, which can be used to identify well bore failure, natural fractures and sedimentary features. The image logs interpreted in this study were run with conventional log suits whilst drilling the well (prior to the mini-frac injections). Two main classes of rock-fabric were identified on image logs in the Cooper Basin (Fig. 8). These were

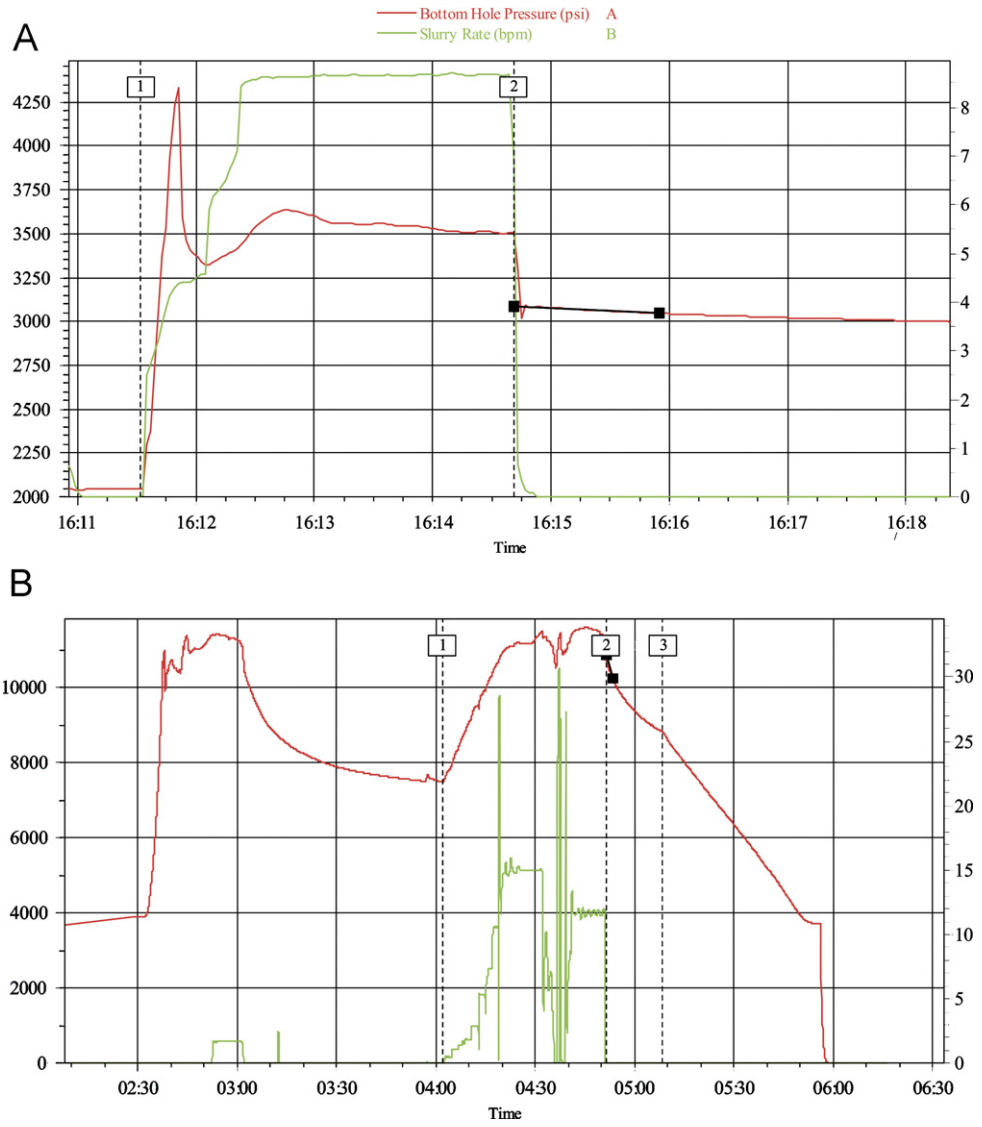

Fig. 4. Pressure versus time records for fracture stimulation treatments in B6 (A) and B54 (B). The B6 was treatment was simple and required a low treating pressure. The B54 well was difficult to frac and required a very high treating pressure.

sparsely spaced natural fractures and a sub-horizontal to gently dipping fabric (interpreted to be 'unloading' fractures). In some wells, the 'fabrics' were interpreted to be open and hydraulically conductive in the near-well bore environment. This interpretation was based on the observation that the fabrics were electrically conductive (due to the invasion of conductive drilling mud) and appeared dilated and 'washed out' with irregular (non-planar) surfaces. The dilated fabrics are held open by the perturbed near well bore stress concentration that is created by the removal of rock during drilling [39,40].

Natural fractures were observed on image logs in four of the 13 treatment zones analysed as part of this study (Table 1). Electrically conductive and resistive fractures were interpreted on the image logs and were sparsely spaced in all treatment zones. The natural fractures are variably oriented, dip between 40° and 80°, and are believed to have formed in response to local stresses.

The second class of fabric was a sub-horizontal to gently dipping (0–25°) fabric that occasionally cut bedding and was identified in eight of the 13 treatment zones. The fabric was interpreted to be open and dilated at the well bore wall (Fig. 8; Table 1). The exact nature of the fabric is unclear, although we believe it is the horizontal tensile microfractures that have been observed in core and thin section in the Cooper Basin [41]. The microfractures have been shown to selectively part causing core discing on unloading and are observed to cut quartz grains in thin sections (Fig. 9). Flottmann et al. [41] link the horizontal microfractures to unloading and exhumation during a period of tertiary thrusting in the Cooper–Eromanga Basin. Flottmann et al. [41] show that the microfractures are widely spread and can be correlated with regions of highest exhumation in the Cooper basin. The fractures can also be associated with difficulties in fracture stimulation operations [41].

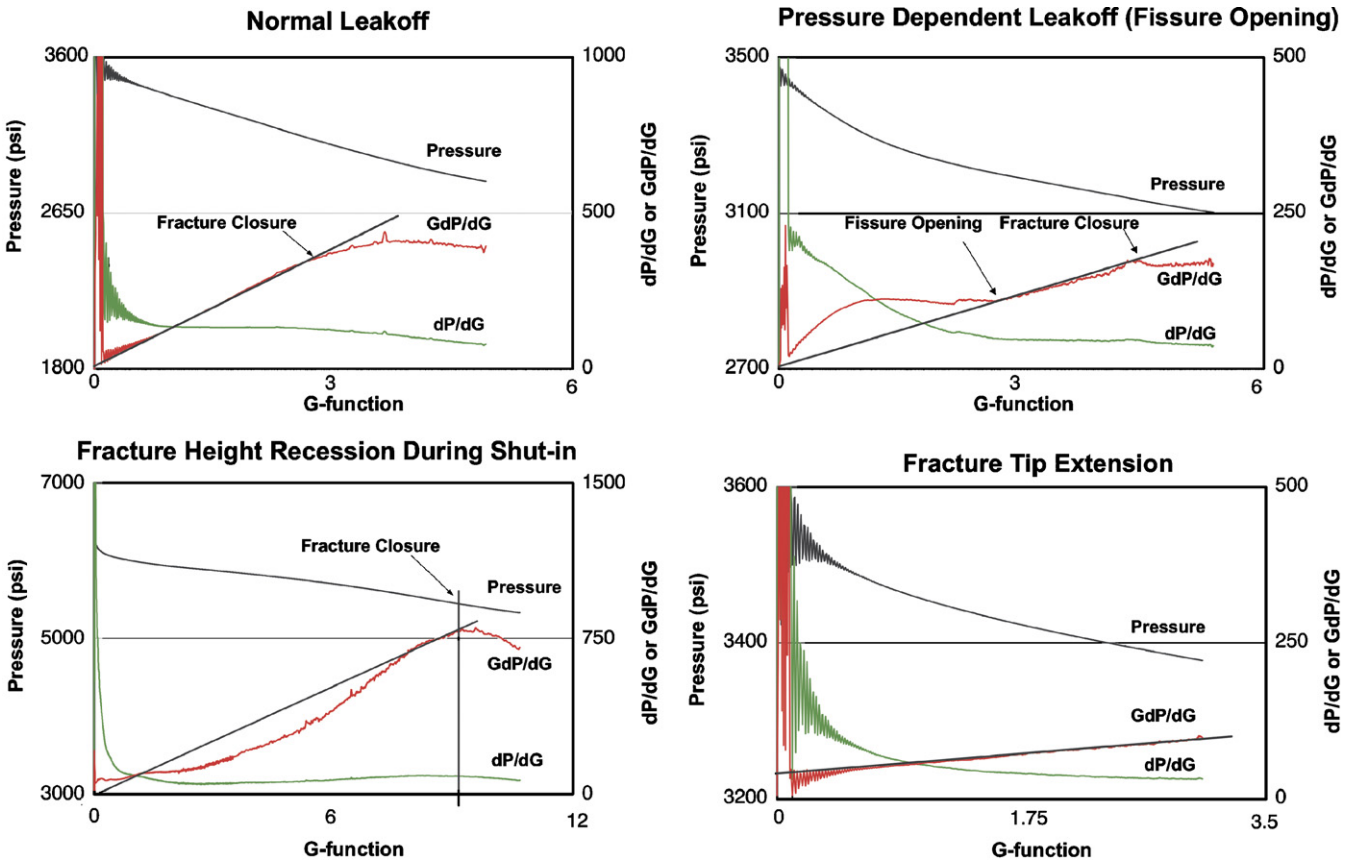

Fig. 5. G-function derivative analysis of leak-off mechanisms (modified from [38]).

5. Tensile rock strength in the Cooper Basin

Tensile (Brazilian) rock strength testing was undertaken on 34 samples from seven of the 13 treatment zones by CSIRO (Table 1). The samples were vacuum-saturated to 30% with 10000 ppm NaCl brine then jacketed with a flexible rubber membrane and installed in the Brazilian cell. The samples were loaded axially until failure. Results of the tensile rock strength testing indicate that reservoir rocks in the Cooper Basin have tensile strengths of 3.8–15.1 MPa (551–2176 psi; Table 1).

Whilst laboratory rock strength testing at atmospheric conditions is not always representative of rock strength at reservoir depth and temperature, the Brazilian rock strength testing indicates significant variation in rock strength between treatment zones. Treatment zones where mini-frac injections measured significant hydraulic fracture complexity (high ISIP, NWBPL and P_{net}) were associated with tensile strengths of greater than 7 MPa (1015 psi; Table 1). Treatment zones in which pressure declines suggest simple fracture propagation were associated with tensile strengths of less than 4 MPa (580 psi). The tensile strength of reservoir rock in the Cooper Basin is noteworthy as in most geomechanical studies the tensile strength of rock is assumed negligible [24,42].

6. Relationship between the tensile strength, rock fabric, in situ stress and measured closure stress (P_c)

Analysis of geological fabrics (from image logs), mini-frac pressure records and tensile rock strength tests from the 13 treatment zones studied herein, and knowledge of the in situ stress tensor from the observation of dilated horizontal fabrics (discussed below and in Appendix), suggest that there are three 'Types' of treatment zone in the Cooper Basin (Tables 1 and 2).

6.1. Type 1 reservoirs

Type 1 reservoirs are characterised by high P_{net}, high NWBPL, pressure-dependent leak-off (PDL) and high closure pressures (an average of 22.4 MPa/km; 0.99 psi/ft), suggesting that injections in these reservoirs result in a complex, hydraulic fracture network (Table 1). This hypothesis is corroborated by the image logs, which show numerous fabrics, dilated at the well bore wall, which may have contributed to the complex initiation and propagation of hydraulic fractures. In seven of the eight reservoirs investigated the closure pressure exceeds the overburden stress (typically less than 21.5 MPa/km; 0.95 psi/ft). Hence the hydraulic fracture is not opening or closing against the least principal stress. Given that the injection tests are

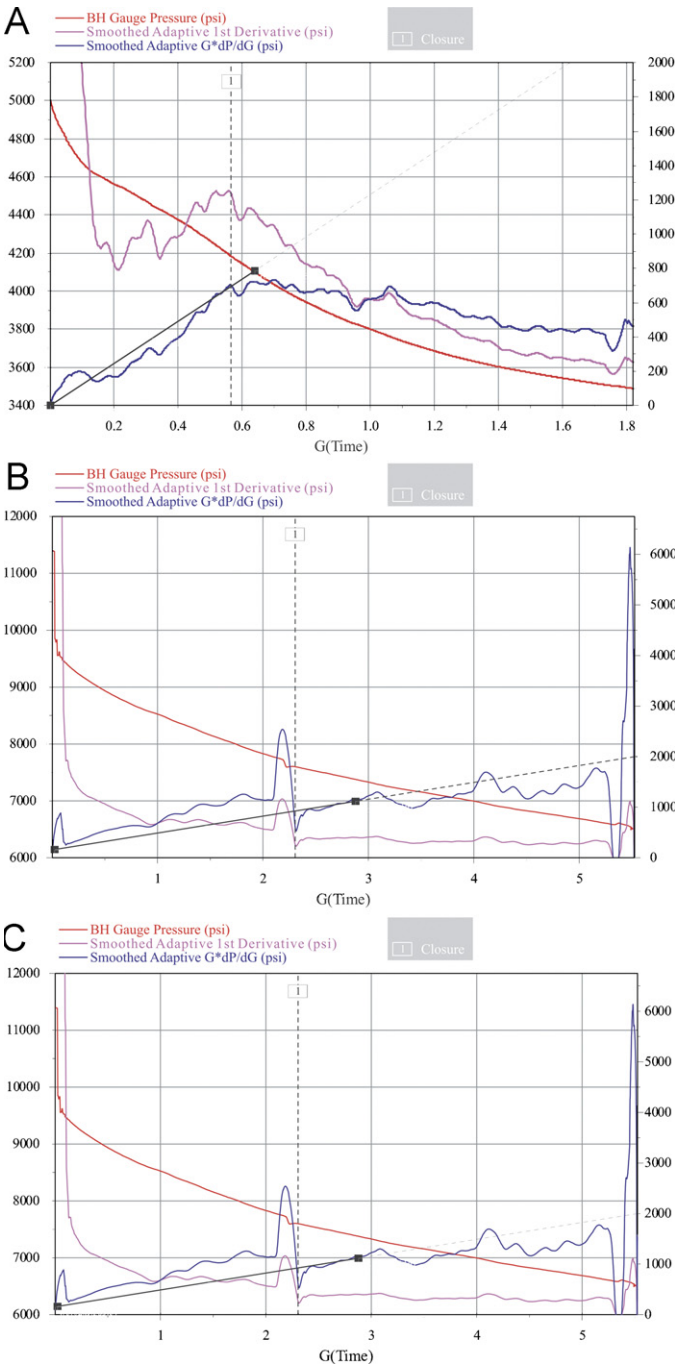

Fig. 6. (A) A simple decline profile for picking P_c (obtained from well P11) with the selection made at a pressure of 4185 psi (33.2 MPa). The time of the closure pressure is identified by the dotted vertical bar. The bottom hole pressure is given in red, the first derivative in purple and the superposition derivative in dark blue. (B) and (C) A difficult decline profile for picking P_c (obtained from well M72)—the two plots show a range of possible outcomes from 7600–6651 psi (52.4–45.9 MPa). The time of the closure pressure is identified by the dotted vertical bar in each case. The bottom hole pressure is given in red, the first derivative in purple and the superposition derivative in dark blue.

demonstrating that hydraulic fractures are not opening against the least principal stress, alternate means must be used to determine S_{hmin} (Appendix). Analysis of the in situ stress regime required to open and dilate horizontal fabrics

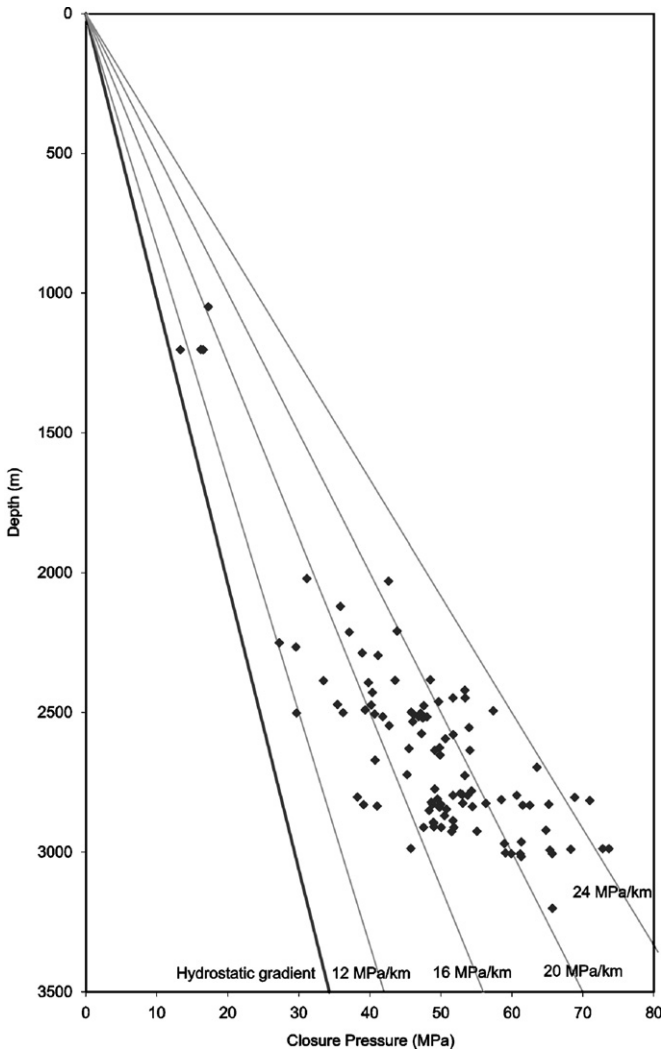

Fig. 7. Mini-frac closure pressures interpreted using the methodology from [34] in the Cooper Basin.

(with no tensile strength) in the near-well bore environment found that S_{hmin} could be as low as 18.1 MPa/km or 0.80 psi/ft (Appendix). This independent estimate of S_{hmin} is significantly lower than the interpreted closure stress (an average of 22.4 MPa/km; 0.99 psi/ft) in the 'Type 1' reservoirs and is consistent with our hypothesis that P_c is not yielding S_{hmin}.

We propose that the contrast in tensile strength between intact rock (>7 MPa/1015 psi) and pre-existing weaknesses in the reservoir (fabric identifiable from image log assumed to be $T = 0$) within a strike-slip stress regime (i.e., lower bound $S_{hmin} \approx 18.1$ MPa/km/0.8 psi/ft), is the mechanism which allows hydraulic fluid to propagate along multiple fracture pathways during mini-frac injections in 'Type 1' reservoirs. The combination of in situ stress, geological weaknesses inherent in the reservoir and high intact rock tensile strength leads to closure pressures that differ significantly from the true value of S_{hmin}.

Comparing the measured closure pressures with the expected normal stress incident on a fracture plane using

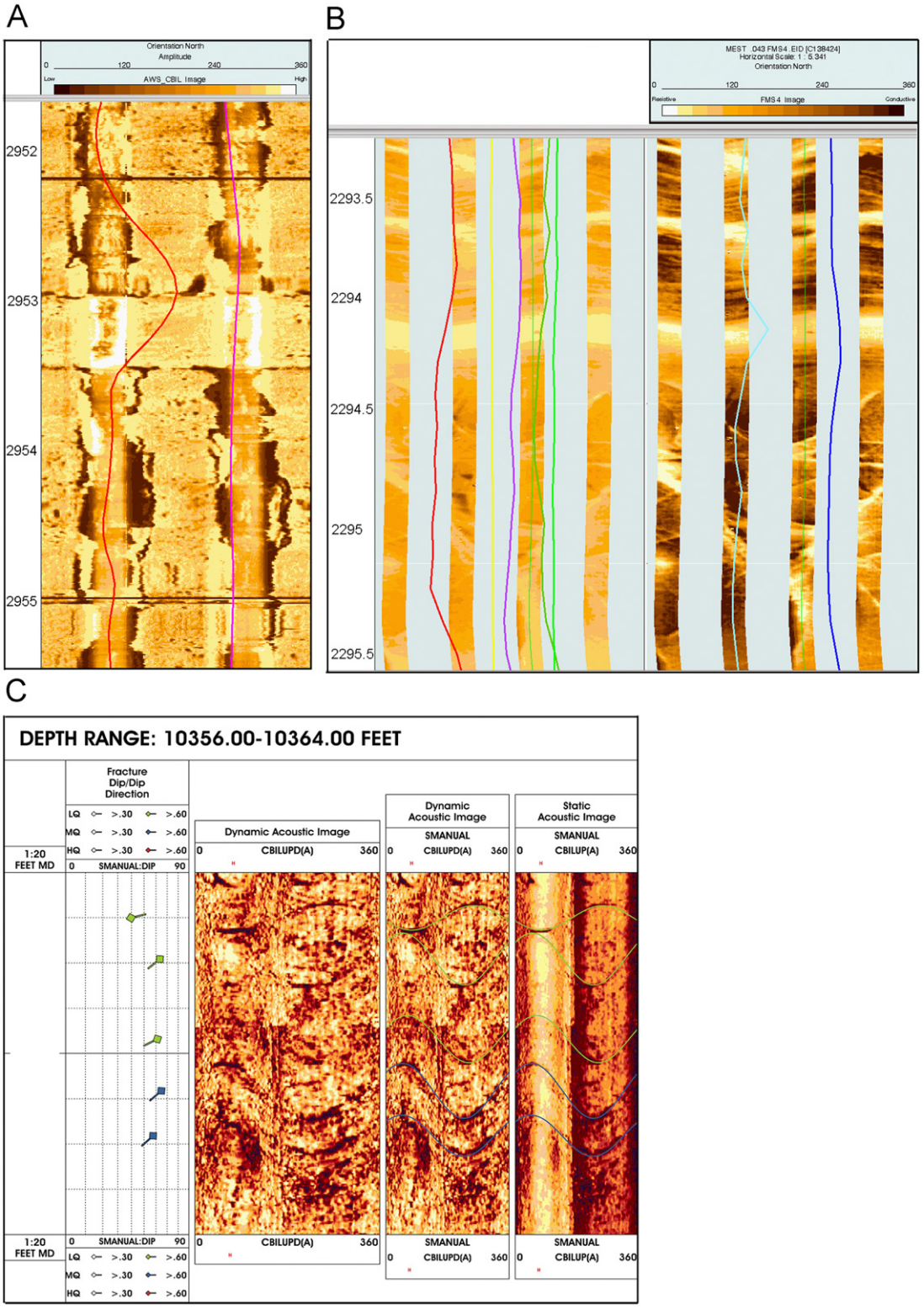

Fig. 8. Fabrics observed in the Cooper Basin image logs. (A) An example of a sub-horizontal fabric believed to be related to tertiary unloading in the Cooper Basin. (B and C) Examples of natural fractures observed in two of the treatment zones interpreted. The images in (A) and (C) are from acoustic image log tools and (C) is from a resistivity image log tool. (B) shows a static image on the left and the dynamic image on the right.

the known in situ stress tensor supports this interpretation (Fig. 10). The normal stress incident on fracture planes oriented vertically (medium thickness sinusoid); on those striking parallel to S_{hmin} (thick sinusoid); and on those striking parallel to S_{Hmax} (thin sinusoid) have been plotted on Fig. 10. The normal to a vertical plane striking parallel

Table 1
Summary of results from analysis of image logs, mini-frac and main-frac pressure records and tensile rock strength testing

	Well	Formation	Complexity observed on image logs	Complexity measured during mini-frac	Depth (to perf midpoint)	P_c (MPa/km)	Vertical stress (MPa/km)	T (MPa)	Treating pressure (MPa/km)	NWBPL (psi)	*P*net
Type 1	SL5	PA	Dilated sub-horizontal fabric	High NWBPL, high P_{net}, PDL	2932	21.7	20.4	7.1	38.1	772	1413
	SL5	TI	Dilated sub-horizontal fabric	High NWBPL, high P_{net}	3006	22.2	21.5	7.15	29.4	1215	1577
	M73	PA	Dilated sub-horizontal fabric, dilated cross bedding & natural fractures	High NWBPL, high P_{net}, PDL	2932	20.4	20.4	15.1	N/A	826	2901
	SL4	PA	Dilated sub-horizontal fabric	High P_{net}, PDL	2818	21.7	20.4	N/A	31	Surface pressure	1413
	SL4	TI	Dilated sub-horizontal fabric	High NWBPL, high P_{net}, PDL	2993	22.6	21.5	N/A	31.7	856	1577
	B54	PA	Dilated sub-horizontal fabric, dilated cross bedding & natural fractures	High NWBPL, high P_{net}, PDL	3024	21.7	20.4	N/A	N/A	646	1058
	DN15	PA	Dilated sub-horizontal fabric, dilated cross bedding and natural fractures	High NWBPL, high P_{net}, PDL	2500	24.2	20.4	N/A	N/A	650	1421
	DN18	PA	Dilated sub-horizontal fabric, dilated cross bedding and natural fractures	High NWBPL, high P_{net}, PDL	2640	23.8	20.4	N/A	N/A	2000	2814
Type 2	M73	TO	None	None	2561.5	18.6	20.4	7.8	N/A	None	127
	M74	TO	None	None	2533	19.0	20.4	8.4	23.3	None	
Type 3	B6	MU	None	None	1199	16.1	20.4	4.3	17.2	None	294
	Br3	PA	None	None	2844	15.4	20.4	N/A	22.6	256	980
	P11	TI	None	None	2265	13.1	20.4	3.8	20.6	270	848

'PA' represents the Patchawarra formation, 'TI' represents the Tirrawarra formation, 'TO' represents the Toolachee formation and MU represents the Murta formation. 'NWBPL' is near-wellbore pressure loss, 'P_{net}' is net stress, 'P_c' refers to closure pressure and 'T' to intact rock tensile strength.

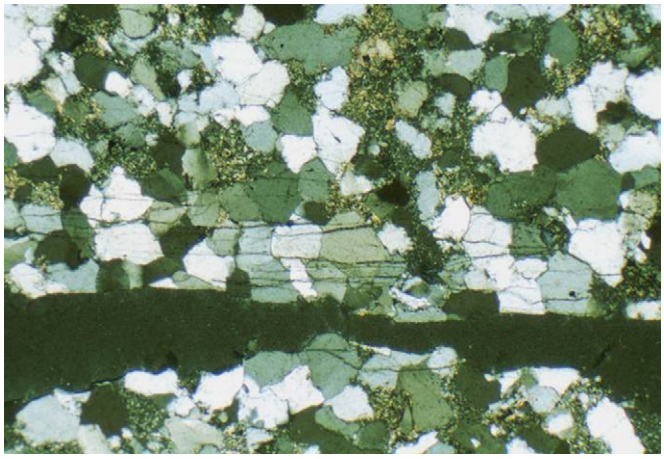

Fig. 9. Thin section of sub-horizontal microfractures cutting quartz grains.

Table 2
'Types' of treatment zones determined from analysis of mini-frac pressure records, image logs, tensile rock strength tests and knowledge of the in situ stress tensor

Type	Observations
Type 1	Closure pressures >0.95 psi/ft Hydraulic fracture complexity observed during injection tests Natural fractures and sub-horizontal 'unloading fractures observed on image logs
Type 2	Closure pressures $\sim$0.84 psi/ft No hydraulic fracture complexity observed during injection tests No weak geological fabrics observed on image logs
Type 3	Closure pressures <0.84 psi/ft No hydraulic fracture complexity observed during injection tests No weak geological fabrics observed on image logs

to S_{hmin} plots at 'A' on the thick sinusoid. The normal to a vertical plane striking parallel to S_{Hmax} plots at 'B' on the medium sinusoid. The normal stress acting on the sub-horizontal fabrics seen on the image logs is consistent with the average measured P_c in 'Type 1' reservoirs.

It has previously been mentioned that some closure pressures are difficult to define on G-function plots from the mini-frac pressure decline. Some of the complexity may result from the fact that a pressure decline does not exhibit one single closure pressure but rather multiple events. To more broadly assess the types of fabrics that could be opening, one can use the actual treating pressures observed during the treatment since these provide an upper limit to the normal stresses that could be exhibited on pre-existing fabrics. The treating pressures attained during fracture stimulation operations in the Cooper Basin are significantly higher than the interpreted closure pressures (Table 1). This is particularly true of treatments in the in the 'Type 1' reservoirs where the average treating pressure is 32.1 MPa/km (1.42 psi/ft). This suggests that even fabrics aligned close to S_{Hmax} may be reactivated during hydraulic fracture operations. The average treating pressure for the 'Type 1' reservoirs has been plotted on Fig. 10. If the average treating pressure gradient is assumed, the normal stress on any plane of weakness dipping towards S_{hmin} would be exceeded. Similarly, the normal stress on fractures dipping less than 50° towards S_{Hmax}, and vertical fractures striking within 48° of S_{Hmax} (090°N) could also be dilated during fracture stimulations in 'Type 1' reservoirs.

6.2. Type 2 reservoirs

Treatments in 'Type 2' reservoirs are characterised by high measured tensile strength (>7 MPa/1015 psi) and high closure pressure ($P_c>18.1$ MPa/km/0.8 psi/ft), however there is no hydraulic fracture complexity as measured by P_{net}, PDL or NWBPL. The closure pressures measured in the 'Type 2' treatment zones are $\sim$18.6–19.0 MPa/km (0.82–0.84 psi/ft). When the image logs for these reservoirs are investigated, no geological weaknesses are apparent. We propose that where wells do not intersect pre-existing geological weaknesses (here natural fractures or sub-horizontal 'unloading' fabrics) ideal simple, bimodal fractures perpendicular to S_{hmin} initiate. Hence, it is considered that the closure pressures measured in 'Type 2' reservoirs are representative of S_{hmin}. The occurrence on image logs of geological weaknesses where P_{net}, PDL and NWBPL indicate hydraulic fracture complexity and their absence from image logs where P_{net}, PDL and NWBPL are not observed and hence do not indicate complexity, is a critically important observation to our interpretation.

6.3. Type 3 reservoirs

'Type 3' reservoirs are characterised by low tensile strength (<4 MPa/580 psi) and low closure pressures (<17 MPa/km/0.75 psi/ft). No hydraulic fracture complexity (i.e., no P_{net}, PDL or NWBPL) or pre-existing geological weaknesses are observed in the 'Type 3' treatment zones and hence measured closure pressures are believed to be representative of S_{hmin}. The low tensile strength of the 'Type 3' reservoirs may help facilitate the initiation of a simple, bimodal tensile fracture at the well bore wall.

6.4. The relationship between closure pressure and hydraulic fracture complexity

The above analysis of the 13 treatment zones and analysis of the horizontal in situ stresses independently of mini-frac data (Appendix) has shown that closure pressure does not necessarily represent a minimum principal stress in areas where hydraulic fracture complexity is measured. This is particularly evident where P_c exceeds S_v. Fig. 12 is a plot of P_c versus P_{net} (far-field hydraulic fracture complexity). The figure shows that as P_c increases, the fracture complexity as measured by P_{net} also increases. High net

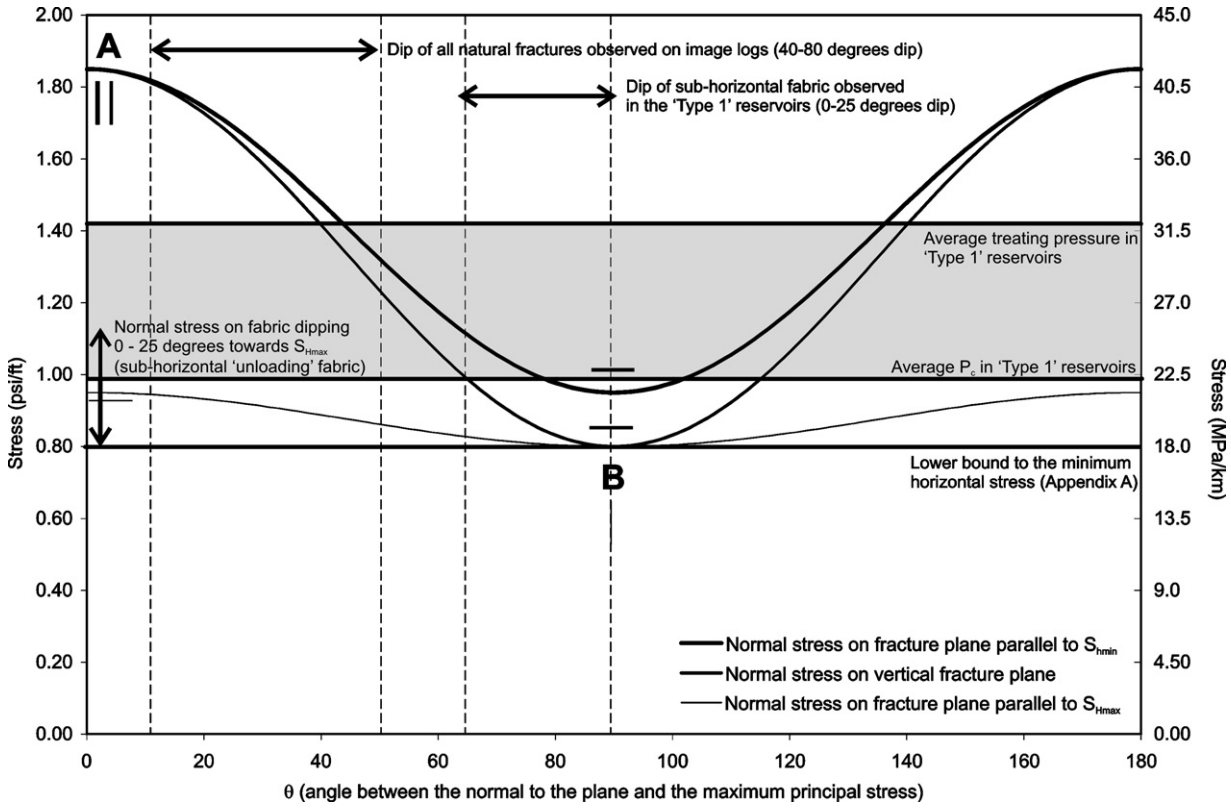

Fig. 10. Normal stress acting on weak geological planes oriented vertically (green) and striking parallel to S_{Hmax} (blue) and S_{hmin} (pink) assuming $S_v = 21.5$ MPa/km, $S_{Hmax} = 42$ MPa/km, $S_{hmin} = 18.1$ MPa/km and $v = 0.24$. The figure shows that the normal stresses on dipping geological weaknesses (sub-horizontal unloading fractures and steeply dipping fractures) can account for the high closure pressures measured in the Cooper Basin. The figure also shows that the average treating pressures in 'Type 1' reservoirs are very high and exceed the normal stress on most planes except those most closely aligned with the S_{hmin} orientation. This means that multiple hydraulic pathways are likely to be utilised during fracture stimulation treatments resulting in high measured complexity.

pressures (interpreted as greater than 6.9 MPa/1000 psi) occur at closure pressures of approximately 19.0 MPa/km (0.84 psi/ft) or greater. Values of net stress that exceed 6.9 MPa (1000 psi) are typically difficult to understand using typical linear elastic, bi-models fracture models [personal communication with Mike Smith NSI Technologies] and may therefore be consistent with the complex networks of hydraulic fractures previously discussed. The apparent 'cut-off' between complex and simple hydraulic fracture geometry of ~19 MPa/km (0.84 psi/ft) in Fig. 11 is consistent with the approach described in Appendix, which contends that this is approximately the value of S_{hmin} required to dilate the sub-horizontal fabrics at the well bore wall prevalent in some areas of the Cooper Basin.

7. Constraining S_{hmin} in the Cooper Basin

The assessment of rock fabric, tensile strength and closure pressures in the Cooper Basin suggests that closure pressures from mini-fracs in Type 1 reservoirs are unlikely to represent S_{hmin} as the hydraulic fracture does not close against the minimum principal stress. The hydraulic fluid is believed to propagate along pre-existing sub-horizontal fractures that can open and act as conduits for hydraulic fluid when the minimum horizontal stress is greater than 85% of S_v and the tensile strength of the rock is less than 8 MPa. The minimum horizontal stress may be less than 85% of S_v if the tensile strength of the rock is greater than 8 MPa (Appendix; Fig. 12). Analysis of rock fabric, tensile strength and closure pressures from the Types 2 and 3 reservoirs suggest that the mini-frac closure pressures are representative of S_{hmin} and that S_{hmin} is between 65% and 80% of S_v.

The analysis above indicates that the minimum horizontal stress varies from ~65–85% of S_v. This is less than would be predicted if only mini-frac closure pressures were considered as has been the case in several other studies of the Cooper Basin. However, the variability is still significant. One possibility for this variation is that it reflects stress heterogeneity between different rock units [10,43,44]. Plumb [10] found that the ratio of minimum to vertical present-day stress was 40% greater in 'hard' carbonate rocks, and 20% higher in 'hard' sandstones, than in the 'weak' shales in sedimentary basins at high present-day stress (reverse stress regimes). Similarly, the ratio of minimum to vertical stress was found to be 4–15% higher in 'weak' shales than in 'strong' sandstones in basins in a relaxed present-day stress state (normal fault regimes). Other authors, including Warpinski and Teufel [43] and Evans and Engelder [44], also report lithology-related

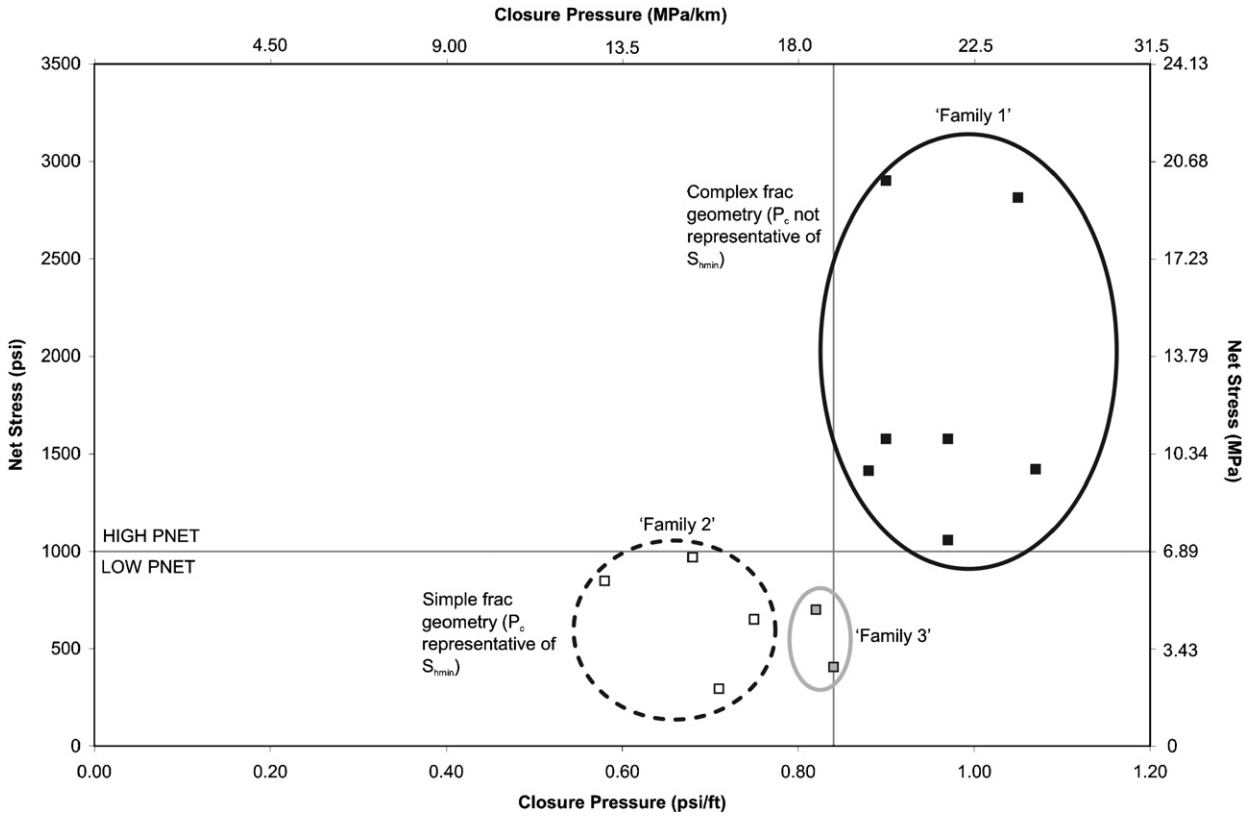

Fig. 11. Plot of P_{net} versus P_c using data from the 13 treatment zones analysed herein. The plot shows that closure pressures above 19 MPa/km (0.84 psi/ft) are associated with net stresses (far-field hydraulic fracture complexity) above 6.9 MPa (1000 psi).

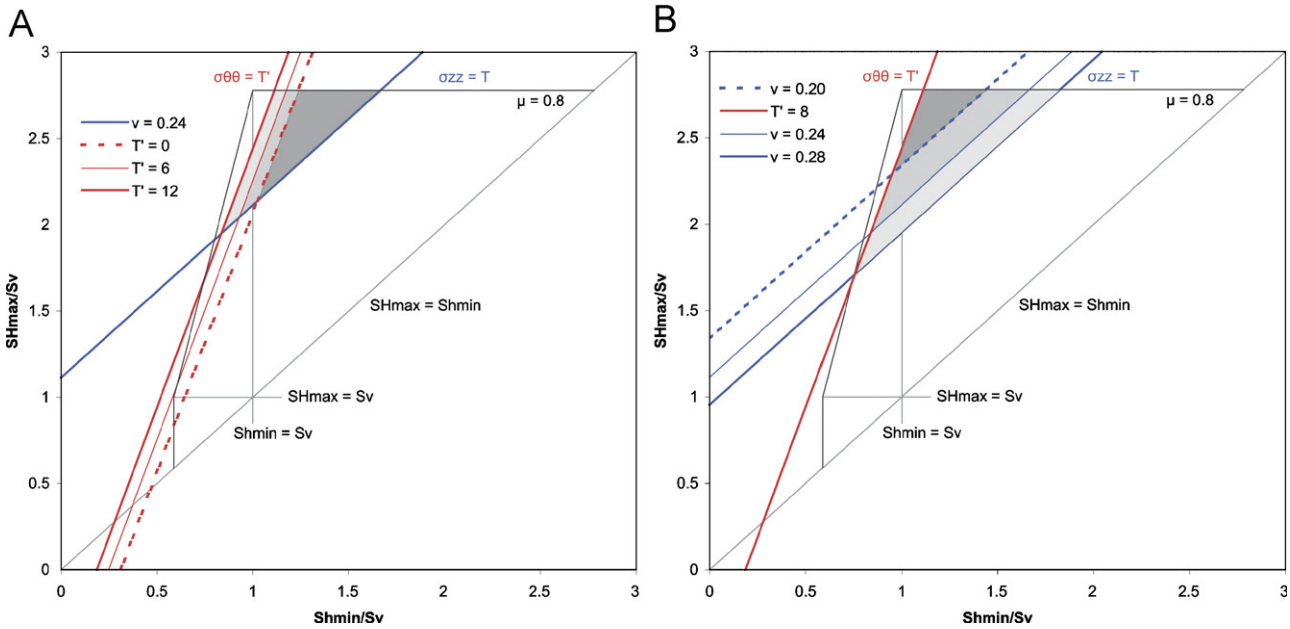

Fig. 12. (Left) Allowable region diagram showing the stress conditions under which horizontal fabrics may open (and/or be created) in the Cooper Basin. The tensile strength of the horizontal planes is assumed zero. The vertical tensile strength is varied (0, 6 and 12 MPa). S_v was assumed ~21.5 MPa/km (0.95 psi/ft). P_w and P_p were assumed–hydrostatic. (Right) Allowable region diagram showing the effect of Poisson's ratio on the allowable region for opening horizontal fabrics at the well bore wall. The tensile strength of the horizontal planes is assumed zero. The vertical tensile strength is assumed 8 MPa. S_v was assumed ~21.5 MPa/km (0.95 psi/ft). P_w and P_p were assumed hydrostatic.

stress variations between different units. The results of tensile rock strength testing in the Types 1–3 reservoirs showed that the strength of the different units is quite large and as such it is quite likely that the variation in S_{hmin} suggested by the analysis above is real and that stress partitioning occurs in the Cooper Basin.

8. Conclusions

Closure pressures interpreted from mini-frac injection tests conducted prior to fracture stimulation treatments are normally considered reliable indicators of the minimum principal stress magnitude. However, the combination of high in situ stress, high intact tensile rock strength and the presence of weak geological fabrics in some areas of the Cooper Basin result in complex hydraulic fracture propagation in which the measured closure pressure is not representative of the minimum principal stress magnitude. The key observations that support this interpretation are:

- the observation of geological weaknesses in reservoirs in which P_{net}, PDL and NWBPL (from injection tests) indicate hydraulic fracture complexity,
- the absence of geological weaknesses in the same reservoirs in which P_{net}, PDL and NWBPL (from injection tests) indicate hydraulic fracture complexity, and
- the measurement of closure pressures in excess of S_v and of the interpreted S_{hmin} (Appendix).

In areas of high in situ stress, high intact tensile strength and pre-existing fabrics, the measured closure pressures are believed to be representative of the normal stress incident on pre-existing geological weaknesses exploited by the growing hydraulic fracture. Where tensile rock strength is high and pre-existing weak rock fabrics exist closure pressures from injection tests should be treated with caution. We believe that such scenarios are not uncommon in onshore tight gas plays where injection tests are routinely performed.

Acknowledgements

The authors thank Santos Ltd. for supporting publication of this work, and, in particular, Carl Greenstreet, David Warner, Thomas Flottmann and Keith Boyle for their technical contributions to the ASP/Santos Geomechanical study.

Appendix. Constraining the in situ stress tensor using knowledge of tensile strength and horizontal fabrics at the well bore wall

The analysis undertaken herein suggests that closure pressures in wells with measured hydraulic fracture complexity may not be representative of S_{hmin}. Hence, an alternative method of estimating in situ stress in the Cooper Basin was employed. Horizontal planes that are observed to open and dilate in the near-well bore environment can be used to constrain the in situ stress tensor [25,40]. Tensile failure occurs at the well bore wall when the minimum circumferential stress (stress tangential to the well bore) becomes less than the tensile strength of the rock. The criterion for formation of axial DITFs in elastic, impermeable rocks in vertical well bores can be represented by:

$$\sigma_{\theta\theta min} = 3S_{hmin} - S_{Hmax} - P_w - P_p \leqslant T', \quad (1)$$

where $\sigma_{\theta\theta min}$ is the minimum circumferential stress, S_{hmin} and S_{Hmax} are total stresses, P_w is the mud weight, P_p is the pore pressure, and T' is the tensile strength of the rock to horizontal loading [45,46]. Assuming elastic impermeable rocks, two criteria must be met to facilitate the opening of pre-existing horizontal fabrics (weaknesses) in tension:

(1) The axial well bore stress must be less than or equal to the tensile strength of the horizontal fabric (T). In most cases, the tensile strength of bedding planes and fractures is much less than that of the intact rock and can be assumed negligible ($\sigma_{zz} \leqslant 0$).
(2) The circumferential stress must be greater than the tensile strength (T') of the intact rock to horizontal loading, precluding the formation of vertical DITFs.

The axial stress around the well bore can be written:

$$\sigma_{zzmin} = S_v - 2\nu(S_{Hmax} - S_{hmin}) - P_p. \quad (2)$$

Assuming horizontal fabrics open when $\sigma_{\theta\theta} \geqslant T'$ and $\sigma_{zzmin} \leqslant T$, and the strength of pre-existing fabrics/weaknesses (T) is negligible, Eqs. (1) and (2) can be re-written as

$$\sigma_{\theta\theta min} = 3S_{hmin} - S_{Hmax} - P_w - P_p \leqslant T', \quad (3)$$

$$\sigma_{zzmin} = S_v - 2\nu(S_{Hmax} - S_{hmin}) - P_p \leqslant 0. \quad (4)$$

Eqs. (3) and (4) can be used to determine the upper and lower bounds to S_{Hmax} where horizontal fabrics are observed to be open on image logs in vertical wells and where T, T', S_v, S_{hmin}, P_w and ν can be determined from wire line log data and rock strength testing.

The range of possible relative principal stress magnitudes for normal, strike-slip and reverse faulting environments can be visualised on an allowable region diagram [47,48]. The allowable stress conditions for a particular geographic region are assumed to lie within an area defined by frictional limits (Fig. 12). Frictional limit theory states that the magnitude of S_{Hmax} can be constrained in strike-slip and reverse faulting environments by assuming that the ratio of the maximum to minimum effective stress cannot exceed the magnitude required to cause faulting on an optimally oriented pre-existing fault [22]. The frictional limit to stress is given by

$$\frac{S_1 - P_p}{S_3 - P_p} \leqslant \left[\sqrt{(\mu^2 + 1)} + \mu\right]^2, \quad (5)$$

where μ is the coefficient of friction on an optimally oriented pre-existing fault, S_1 is the maximum principal stress, and S_3 is the minimum principal stress. The above equation effectively states that if the ratio of $(S_1-P_p)/(S_3-P_p)$ exceeds μ, then slip will occur. Hence, frictional limits provide an upper bound to S_{Hmax} where it is the maximum principal stress. Since there is no active faulting in the Cooper Basin, then frictional limits constrain the allowable values of S_{Hmax} to within the black outline in Fig. 12 (where $\mu = 0.8$; the average from rock strength testing). The grey lines representing $S_{Hmax} = S_v$ and $S_{hmin} = S_v$ and separate the normal, strike-slip and reverse fault regimes (Fig. 12) as defined by Anderson [49].

Eqs. (3) and (4) can be plotted as lines on the allowable region diagram facilitating determination of the stress region in which horizontal fabrics might open (Fig. 12). Considering the criterion $\sigma_{\theta\theta min} \geqslant T'$ (Eq. (3)) and a generalised in situ stress tensor ($S_v \sim 21.5$ MPa/km (0.95 psi/ft), $P_p \sim 9.8$ MPa/km (0.433 psi/ft), $P_w \sim 9.8$ MPa/km (0.433 psi/ft), $T = 0$ MPa and $\nu \sim 0.24$), then allowable values for S_{Hmax} must lie in the region to the right of the red line in Fig. 12. Similarly the criterion $\sigma_{zz} = 0$ (Eq. (4)) constrains the allowable values of S_{Hmax} to the left of the blue line in Fig. 12. The effect of the tensile strength of the rock to horizontal loading (T') and ν on the allowable stress region for opening of horizontal fabrics at the well bore wall is shown in Fig. 12. The observation of open horizontal fabrics on image logs can constrain the lower bound of the stress field to one where $S_{hmin} = 18$ MPa/km (0.80 psi/ft) and $S_{Hmax} = 41.9$ MPa/km (1.85 psi/ft) assuming $T' = 7$ MPa (1015 psi), $\nu = 0.8$, and $\nu \sim 0.24$.

References

[1] Martin CD, Kaiser PK, Christiansson R. Stress, instability and design of underground excavations. Int J Rock Mech Min Sci 2003;40:1027–47.

[2] Tolppanen PJ, Johansson EJW, Riekkola R, Salo J-P. Comparison of vertical and horizontal deposition hole concept for disposal of radioactive waste based on rock mechanical in situ stress-strength analyses. Eng Geol 1998;49:345–52.

[3] Raaen A, Brudy M. Pump-in/flowback tests reduce the estimate of horizontal in situ stress significantly. In: SPE ann tech conf exhibition, New Orleans, 2001, paper SPE 71367.

[4] Smith MB, Shlyapobersky JW. Basics of hydraulic fracturing. In: Economides MJ, Nolte K, editors. Reservoir stimulation. West Sussex, England: Wiley; 2000. p. 5(1)–5(28).

[5] Bell JS. Petro geoscience 1. In situ stresses in sedimentary rocks (part 1): measurement techniques. Geosci Can 1996;23:85–100.

[6] Evans K, Engelder T, Plumb RA. Appalachian stress study 1: a detailed description of in situ stress variation in Devonian shales of the Appalachian Plateau. J Geophys Res 1989;94:1729–54.

[7] Warpinski NR, Brannagan P, Wilmer R. In situ stress measurements at US DOE's multiwell experiment site, Mesaverde Group, Rifle, Colorado. J Pet Technol 1985;37:527–36.

[8] Raaen A, Hovern K, Joranson H, Fjaer E. FORMEL: a step forward in strength logging. In: SPE ann tech conf exhibition, Denver, 1996, paper SPE 36533.

[9] Reches Z. Tensile fracturing of stiff rock layers under triaxial compressive stress states. Int J Rock Mech Min Sci 1998;35:456–7.

[10] Plumb RA. Variations of the least horizontal stress magnitude in sedimentary rocks. In: First North American rock mechanics symposium, Austin. Rotterdam: Balkema; 1994.

[11] Cornet F, Valette B. In situ stress measurement from hydraulic fracture injection test data. J Geophys Res 1984;89:11527–37.

[12] Iverson WP. Closure stress calculations in anisotropic formations. In: SPE rocky mountain regional/low-permeability reservoirs Conference, Denver, 1995, paper SPE 29598.

[13] Yang Z, Crosby DG, Akgun F, Khurana AK, Rahman SS. Investigation of the factors influencing hydraulic fracture initiation in highly stressed formatons. In: Asia Pacific Oil gas Conference, Kuala Lumpur, 1997, paper SPE 38043.

[14] Reynolds SD, Mildren SD, Hillis RR, Meyer JJ. Constraining stress magnitudes using petroleum exploration data in the Cooper–Eromanga Basins, Australia. Tectonophysics 2005;415:123–40.

[15] Reynolds SD, Mildren SD, Hillis RR, Meyer JJ, Flottmann T. Maximum horizontal stress orientations in the Cooper Basin, Australia: implications for plate scale tectonics and local stress sources. Geophys J Int 2005;150:331–43.

[16] Ludwig WE, Nafe JE, Drake CL. Seismic refraction. In: Maxwell AE, editor. The Sea: Ideas and Observations on Progress in the Study of the Sea. New York: Wiley-Interscience; 1970. p. 53–84.

[17] Mavromatidis A, Hillis R. Quantification of exhumation in the Eromanga Basin and its implications for hydrocarbon exploration. Pet Geosci 2005;11:79–92.

[18] Hillis RR, Meyer JJ, Reynolds SD. The Australian stress map. Exp Geophys 1998;29:420–7.

[19] Gjønnes M, Cruz AMGL, Horsrud P, Holt RM. Leak-off tests for horizontal stress determination? J Pet Sci Eng 1998;20:63–71.

[20] Roberts GA, Chipperfield ST, Miller WK. The evolution of a high near-well bore pressure loss treatment strategy for the Australian Cooper Basin. In: SPE ann tech conf exhibition, Dallas, 2000, paper SPE 63029.

[21] Ito T, Evans K, Kawai K, Hayashi K. Hydraulic fracture reopening pressure and the estimation of maximum horizontal stress. Int J Rock Mech Min Sci 1999;36:811–26.

[22] Sibson RH. Frictional constraints on thrust, wrench and normal faults. Nature 1974;249:542–4.

[23] Bell JS, Gough DI. Northeast-southwest compressive stress in Alberta—evidence from oil wells. Earth Planet Sci Lett 1979;45:475–82.

[24] Brudy M, Zoback MD. Drilling-induced tensile wall-fractures: Implications for determination of in situ stress orientations and magnitudes. Int J Rock Mech Min Sci 1999;36:191–215.

[25] Nelson EJ, Meyer JJ, Hillis RR, Mildren SD. Transverse drilling-induced tensile fractures in the West Tuna area, Gippsland Basin, Australia: implications for the in situ stress regime. Int J Rock Mech Min Sci 2005;42:361–71.

[26] Cleary MP, Johnson DE, Kogsboil H-H, Owens KA, Perry KF, de Pater CJ, et al. Field implementation of proppant slugs to avoid premature screenout of hydraulic fractures with adequuate proppant concentration. In: Rocky mountain regional/low permeability reservoirs symposium, Denver, 1993, paper SPE 25892.

[27] Nolte K. Application of fracture design based on pressure analysis. SPE Prod Eng 1988;31–42.

[28] Thiercelin MC, Rogiers JC. Formation characterisation: rock mechanics. In: Economides MJ, Nolte K, editors. Reservoir stimulation. West Sussex, England: Wiley; 2000. p. 3(1)–3(35).

[29] Wright CA, Minner WA, Weijers L, Davis EJ, Golich GM, Kikuchi H. Well bore-to-fracture communication problems pose challenges in California diatomite horizontal wells. In: SPE ann tech conf exhibition, San Antonio, 1997, paper SPE 38632.

[30] Fjær E, Holt RM, Horsrud P, Raaen AR, Risnes R. Petroleum related rock mechanics. Amsterdam: Elsevier; 1992.

[31] Gu H, Elbel JL, Nolte KG, Cheng AH, Abousleiman Y. Formation permeability determination using impulse-fracture injection. In: SPE prod oper symp, Oklahoma, 1993, paper SPE 25425.

[32] Nolte KG. Principles for fracture design based on pressure analysis. SPE Prod Eng 1998;Feb:22–30.
[33] Castillo JL. Modified fracture pressure decline analysis including pressure-dependent leakoff. In: SPE/DOE low permeability reservoirs symposium, Denver, 1987, paper SPE 16417.
[34] Mukherjee H, Larkin S, Kordziel W. Extension of fracture pressure decline curve analysis to fissured formations. In: SPE rocky mountain regional meeting and low permeability reservoirs symposium, Denver, 1991, paper SPE 21872.
[35] Nolte KG. Determination of fracture parameters from fracturing pressure decline. In: SPE ann tech conf exhibition, Las Vegas, 1979, paper SPE 8341.
[36] Barree B, Mukherjee H. Determination of pressure dependent leakoff and its effect on fracture geometry. In: SPE ann tech conf exhibition, Denver, 1996, paper SPE 36424.
[37] Nolte K. A general analysis of fracturing pressure decline with application to three models. SPE Form Eval 1986:571–83.
[38] Craig DP, Eberhard MJ, Barree RD. Adapting high permeability leakoff analysis to low permeability sands for estimating reservoir engineering parameters. In: SPE rocky mountain regional/low permeability reservoirs symposium, Denver, 2000, paper SPE 60291.
[39] Kirsch G. Die Theorie der Elastizitat und die Beaurforisse der Festigkeitslehre. Zeit Verein Deutsch Ing 1898;42:797–807.
[40] Jaeger JC, Cook NGW. Fundamentals of rock mechanics. 3rd ed. London: Chapman & Hall; 1979.
[41] Flottmann T, Campagna DJ, Hillis R, Warner D. Horizontal microfractures and core discing in sandstone reservoirs, Cooper Basin, Australia. In: PESA Eastern Australasian basins symposium II, Adelaide, 2004.
[42] Byerlee J. Friction of rocks. Pure Appl Geophys 1978;116:615–26.
[43] Warpinski N, Teufel LW. In situ stress in low permeability non-marine rocks. J Pet Technol 1989;April:405.
[44] Evans K, Engelder T. Some problems in estimating horizontal stress magnitudes in ''thrust'' regimes. Int J Rock Mech Min Sci 1989;26: 647–60.
[45] Hubbert MK, Willis DG. Mechanics of hydraulic fracturing. AIME Pet Trans 1957;210:153–66.
[46] Peska P, Zoback MD. Compressive and tensile failure of inclined well bores and determination of in situ stress and rock strength. J Geophys Res 1995;100:12791–811.
[47] Zoback MD, Barton CA, Brudy M, Castillo DA, Finkbeiner T, Grollimund BR, et al. Determination of stress orientation and magnitude in deep wells. Int J Rock Mech Min Sci 2003;40: 1049–76.
[48] Moos D, Zoback MD. Utilization of observations of well bore failure to constrain the orientation and magnitude of crustal stresses: application to continental, deep sea drilling project and ocean drilling program boreholes. J Geophys Res 1990;95:9305–25.
[49] Anderson EM. The dynamics of faulting and dike formation with application in Britain. 2nd ed. Edinburgh: Oliver and Boyd; 1951.